



**CHALMERS**  
UNIVERSITY OF TECHNOLOGY

## **Mineralogy of an OH/IR superwind**

Downloaded from: <https://research.chalmers.se>, 2022-06-29 09:52 UTC

Citation for the original published paper (version of record):

Lombaert, R., de Vries, B., Hillen, M. (2016). Mineralogy of an OH/IR superwind. *Journal of Physics: Conference Series*, 728(2). <http://dx.doi.org/10.1088/1742-6596/728/2/022004>

N.B. When citing this work, cite the original published paper.

# Mineralogy of an OH/IR superwind

R. Lombaert<sup>1</sup>, B. L. de Vries<sup>2</sup> and M. Hillen<sup>3</sup>

<sup>1</sup> Chalmers University of Technology, Department of Earth and Space Sciences, Onsala Space Observatory, 439 92 Onsala, Sweden

<sup>2</sup> ESA, Scientific Support Office, Directorate of Science and Robotic Exploration, European Space Research and Technology Centre (ESTEC/SRE-S), Keplerlaan 1, 2201 AZ Noordwijk, The Netherlands

<sup>3</sup> KU Leuven, Instituut voor Sterrenkunde, Celestijnenlaan 200D B-2401, 3001 Leuven, Belgium

E-mail: <sup>1</sup> [robin.lombaert@chalmers.se](mailto:robin.lombaert@chalmers.se)

**Abstract.** The mineralogy of the dense, dusty superwind of OH/IR stars can provide important constraints for understanding the dust formation process as well as the acceleration of the wind. We aim to model the ISO-SWS spectrum of the OH/IR star OH 30.1-0.7 in detail by reproducing the slope of the spectral energy distribution in the continuum regions between 3 and 8  $\mu\text{m}$  and 12 and 15  $\mu\text{m}$ . In addition to metallic Fe, we find that larger amorphous olivine grains of size on the order of 1  $\mu\text{m}$  may also contribute to the continuum emission. We report here on the preliminary model results and discuss their validity given the important assumption of a 1D spherically symmetric stellar wind.

## 1. Introduction

When cool stars with intermediate main-sequence masses (5-8  $M_{\odot}$ ) ascend the asymptotic giant branch (AGB) they form an O-rich outflow with both a dusty and a gaseous component. These objects can lose mass at rates as high as ( $\dot{M} \sim 10^{-4} M_{\odot}/\text{yr}$ ) causing them to be enshrouded by a dense, dusty superwind [1, 2]. Bright hydroxyl (OH) maser emission and strong infrared (IR) dust emission allow them to be classified as OH/IR stars, many of which are long-period (up to 2000 days) Mira pulsators with a luminosity of  $\sim 1-5 \times 10^4 L_{\odot}$ .

The high mass-loss rate and cool stellar atmosphere lead to high-density environments in the inner wind where large amounts of dust can form. Constraints on the dust formation process can be inferred by modelling the mineralogy of the stellar wind. The general shape of the spectral energy distribution (SED) is relatively well understood. Two strong absorption features at 10 and 18  $\mu\text{m}$  indicate the presence of amorphous oxygen-rich silicates, including olivine [3, 4]. Other oxygen-rich minerals have been suggested to contribute in the mid-IR as well, such as alumina [5]. However, an additional source of *continuum* opacity was still needed to explain the lack of visual and near-IR flux from these sources. Kemper et al. (2002) suggested that a small abundance of metallic Fe, a solid-state form of Fe atoms, can readily provide this source of continuum opacity in oxygen-rich environments [6].

Metallic Fe can provide the missing continuum opacity, and can help to reproduce the overall shape of the SEDs of OH/IR stars. However, it remains difficult to reconcile the near-IR slope between 3 and 8  $\mu\text{m}$  with the mid-IR flux between 10 and 30  $\mu\text{m}$ . A second contributor to the continuum opacity that allows to change the near-IR slope can alleviate this issue. Here, we



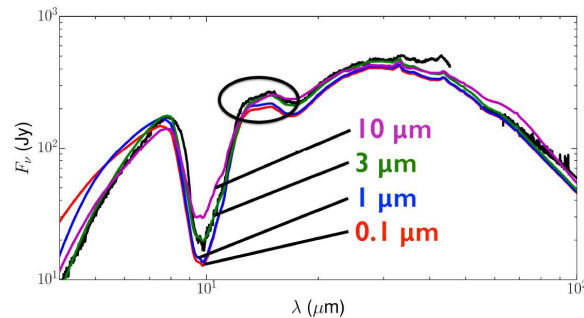


**Figure 1.** The SED of OH 30.1-0.7 is shown in black (ISO-SWS at  $\lambda < 45 \mu\text{m}$  and Herschel-PACS at  $\lambda > 45 \mu\text{m}$ ), overlaid with four models that include olivines with a grain size distribution up to different maximum grain sizes as indicated in the figure. The 12-15  $\mu\text{m}$  region is highlighted.

report on a work in progress to show that micron-sized dust grains can provide a solution. We apply this idea to the dusty stellar wind of the OH/IR star OH 30.1-0.7. The results will be published in an upcoming paper and we refer to that paper for further details.

## 2. Data and Modelling

We use the *Short Wavelength Spectrometer* (SWS) observed with the *Infrared Space Observatory* (ISO) and the *Photodetecting Array Camera and Spectrometer* spectra observed with the *Herschel* telescope, shown in Fig. 1. The relative flux calibration uncertainty between short and long wavelengths in the ISO-SWS spectrum is estimated to be 10%.

We calculate models with the radiative-transfer code *MCMaX*, which self-consistently determines the dust temperature profile and resulting SED [7]. We assume a spherically symmetric expanding stellar wind with a terminal velocity of  $v_{\infty,g} = 18 \text{ km s}^{-1}$ , as constrained by the low-J CO lines observed for this source, and find a mass-loss rate of  $\dot{M}_d = 2.5 \times 10^{-6} M_{\odot}/\text{yr}$ . The outer radius is taken to be 7600 AU to reproduce the relatively low flux in the far-IR. This is in agreement with the short-superwind scenario reported by de Vries et al. 2014 [8], although the size we use is a factor of three larger. The tenuous wind at radii larger than the outer radius of 7600 AU does not contribute significantly to the IR flux. We calculate the pressure-dependent dust condensation temperature for each species [9] and derive an inner radius of the wind of  $R_{i,d} = 22\text{-}45 \text{ AU}$ . The dust is composed of the amorphous olivine  $(\text{Mg}_x\text{Fe}_{1-x})_2\text{SiO}_4$  with  $x = 0.5$  and  $x = 1$ , the amorphous pyroxene  $\text{MgSiO}_3$ , the alumina  $\text{Al}_2\text{O}_3$ , and metallic Fe. For completeness we also include crystalline silicates, i.e. forsterite and enstatite [10], and water ice [11], but these species do not have a significant effect on the overall shape of the SED. We assume an MRN grain size distribution [12] given by

$$\frac{n_d}{da} = A n_H a^{-3.5}, a_{\min} < a < a_{\max} \quad (1)$$

where  $A$  is a constant factor,  $n_H$  is the hydrogen number density and  $a$  is the grain size varying between minimum and maximum values. The minimum grain size is always  $0.01 \mu\text{m}$  and the maximum grain size is varied between  $0.1$  and  $10 \mu\text{m}$ . We use a dust grain shape model given by the distribution of hollow spheres (DHS [13]). The resulting mass extinction opacities are shown in Fig. 2 for metallic Fe and for amorphous olivine with different maximum grain sizes.

## 3. Results and discussion

Preliminary results indicate that metallic Fe alone cannot account for the near-IR slope below  $8 \mu\text{m}$  while remaining consistent with the mid-IR flux between  $10$  and  $40 \mu\text{m}$ . In a first step, we

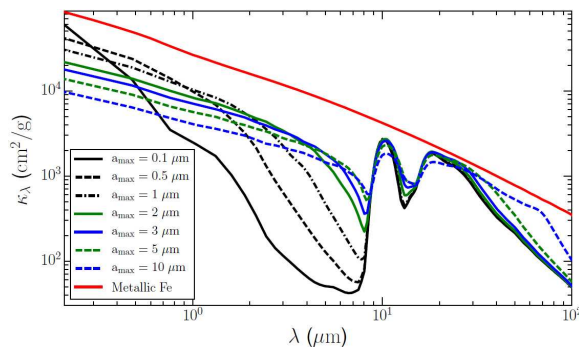


**Figure 2.** Mass extinction opacities as a function of wavelength for metallic Fe (in red) and the amorphous olivine  $(\text{Fe}_{0.5}\text{Mg}_{0.5})_2\text{SiO}_4$  in grain size distributions with several maximum grain sizes (in black, blue and green). The distribution is given by Eq. 1 with a minimum grain size of  $0.01 \mu\text{m}$ .

distinguish between increasing the metallic Fe abundance and increasing the overall dust content through the dust mass-loss rate. For a mass-loss rate of  $2.5 \times 10^{-6} M_{\odot}/\text{yr}$  we derive a metallic Fe abundance of  $(7 \pm 2)\%$  by mass. While this predicts the overall emission reasonably well in the mid-IR and far-IR wavelength region, the near-IR slope is not reproduced. If we increase the maximum size of the amorphous olivine grains to  $1\text{--}5 \mu\text{m}$ , however, we can reproduce the slope much better. Fig. 1 shows the resulting model SEDs for four different maximum grain sizes. These models were not optimised to fit the observations. They illustrate instead the effect of varying the maximum grain size of amorphous olivine.

As highlighted in Fig. 1, the spectral slope in the  $12\text{--}15 \mu\text{m}$  region is also affected by the maximum grain size. The slope in the ISO-SWS observations compares well to that measured by the *Infrared Astronomical Satellite*. Moreover, the ISO-SWS spectrum between  $12$  and  $15 \mu\text{m}$  is measured within a single subband of the spectrometer. The slope in this short wavelength region is thus very reliable. Two model properties affect this slope. First, the slope at a certain wavelength is significantly affected by the maximum grain size only when the Rayleigh limit is not applicable anymore, i.e. when the maximum grain size becomes similar to or larger than that wavelength. While for smaller grains the  $12\text{--}15 \mu\text{m}$  region is not affected, the slope does change for maximum grain sizes of  $1 \mu\text{m}$  or larger. This translates to a slope change in the SED. Second, the inclusion of  $\text{Al}_2\text{O}_3$  in the dust composition changes this slope. However, when including an  $\text{Al}_2\text{O}_3$  abundance in line with the solar abundance, the amorphous silicate still dominates the emission at  $12\text{--}15 \mu\text{m}$ . As a result, the only way to reproduce the  $12\text{--}15 \mu\text{m}$  slope is to include a grain size distribution with a maximum grain size of  $\sim 1 \mu\text{m}$ .

This result is in agreement with recent theoretical findings regarding wind-driving models of oxygen-rich winds. Grain sizes of at least  $0.2 \mu\text{m}$  are needed to drive even a low mass-loss rate oxygen-rich wind due to the importance of scattering on otherwise nearly transparent silicate grains [14, 15]. Grains of similar size were detected in the extended atmosphere of the low mass-loss rate oxygen-rich AGB star W Hya [16]. Hence, it is possible that grains of  $0.1\text{--}0.5 \mu\text{m}$  in size are common in the stellar winds of oxygen-rich AGB stars. Given the much higher mass-loss rates in OH/IR stars, it may be possible that grains can grow to even larger sizes. Interestingly,  $\mu\text{m}$ -sized grains may also exist in the interstellar medium, even though there is a preference for carbon-based grains rather than silicate grains [17].

Finally, we note that some of our assumptions may affect these results. We model the source with a spherically symmetric stellar wind, which may not be justified for OH 30.1-0.7. Data taken with *MID-infrared Interferometric instrument* at the *Very Large Telescope Interferometer* array indicate that the source appears smaller in the plane of the sky than predicted by our radiative-

transfer models. Further analysis is required to interpret these spatially resolved observations in the context of our models.

#### 4. Conclusions

We make a number of preliminary conclusions regarding the requirements of the dust model to reproduce the ISO-SWS SED of OH 30.1-0.7. These are made under the assumption of one-dimensional spherical symmetry of the wind geometry, the validity of which is being verified in ongoing work.

- (i) Metallic Fe contributes to the *continuum* opacity, but it, alone, cannot account for the slope between 3 and 8  $\mu\text{m}$  and between 12 and 15  $\mu\text{m}$ .
- (ii) A contribution from micron-sized dust grains to the *continuum* opacity is required to reproduce the slope.
- (iii) The silicates are made up of both olivines and pyroxenes. The olivines contain Fe and Mg; only a small abundance of pure-Mg olivines can improve the fit to the 8- $\mu\text{m}$  bump.
- (iv) Assuming solar abundance, a near 100% condensation of Fe, Mg and Si from the gas phase into the solid phase is needed.
- (v) No alumina or other signs of early dust formation are reliably detected.

#### References

- [1] Renzini A 1981 *Physical Processes in Red Giants (Astrophysics and Space Science Library vol 88)* ed I Iben Jr & A Renzini pp 431–446
- [2] Iben Jr I and Renzini A 1983 *Annu. Rev. Astron. Astrophys.* **21** 271–342
- [3] Sylvester R J, Kemper F, Barlow M J, de Jong T, Waters L B F M, Tielens A G G M and Omont A 1999 *Astron. Astrophys.* **352** 587–599
- [4] Suh K and Kim H 2002 *Astron. Astrophys.* **391** 665–674
- [5] Maldoni M M, Ireland T R, Smith R G and Robinson G 2005 *Mon. Not. R. Astron. Soc.* **362** 872–878
- [6] Kemper F, de Koter A, Waters L B F M, Bouwman J and Tielens A G G M 2002 *Astron. Astrophys.* **384** 585–593
- [7] Min M, Dullemond C P, Dominik C, de Koter A and Hovenier J W 2009 *Astron. Astrophys.* **497** 155–166
- [8] de Vries B L, Blommaert J A D L, Waters L B F M, Waelkens C, Min M, Lombaert R and Van Winckel H 2014 *Astron. Astrophys.* **561** A75
- [9] Kama M, Min M and Dominik C 2009 *Astron. Astrophys.* **506** 1199–1213
- [10] de Vries B L, Min M, Waters L B F M, Blommaert J A D L and Kemper F 2010 *Astron. Astrophys.* **516** A86
- [11] Dijkstra C, Dominik C, Hoogzaad S N, de Koter A and Min M 2003 *Astron. Astrophys.* **401** 599–611
- [12] Mathis J S, Rumpl W and Nordsieck K H 1977 *Astrophys. J.* **217** 425–433
- [13] Min M, Hovenier J W and de Koter A 2003 *Astron. Astrophys.* **404** 35–46
- [14] Höfner S and Andersen A C 2007 *Astron. Astrophys.* **465** L39–L42
- [15] Höfner S 2012 *Nature* **484** 172–173
- [16] Norris B R M, Tuthill P G, Ireland M J, Lacour S, Zijlstra A A, Lykou F, Evans T M, Stewart P and Bedding T R 2012 *Nature* **484** 220–222
- [17] Wang S, Li A and Jiang B W 2015 *Astrophys. J.* **811** 38